Surface Science 603 (2009) 3035–3040

Contents lists available at ScienceDirect

Surface Science

journal homepage: www.elsevier.com/locate/susc

Stable hydroxyl network on diamond (0 0 1) via first-principles and MD investigation

H.X. Yang [a,*], L.F. Xu [b], C.Z. Gu [b], Z. Fang [b], S.B. Zhang [c], M. Chshiev [a]

[a] Spintec, CEA, CNRS, UJF, INPG, CEA/INAC, 17, Avenue des Martyrs, 38054 Grenoble, France
[b] Beijing National Laboratory for Condensed Matter Physics, Institute of Physics, Chinese Academy of Sciences, P.O. Box 603, Beijing 100080, China
[c] Department of Physics, Applied Physics, and Astronomy, Rensselaer Polytechnic Institute, Troy, NY 12180, USA

ARTICLE INFO

Article history:
Received 31 March 2009
Accepted for publication 7 August 2009
Available online 21 August 2009

Keywords:
Diamond surface
Hydroxyl network
Stability
First-principles
Adsorption kinetics

ABSTRACT

We systemically studied the OH-terminated diamond (0 0 1) surfaces by first-principles calculations. A set of network structures are investigated, two of them are found to be energetically favored over a recently proposed anti-parallel configuration [S.J. Sque, R. Jones, P.B. Briddon, Phys. Rev. B 73 (2006) 085313]. The transition paths and barriers between the anti-parallel configuration and the network structures are calculated. Furthermore, using *ab initio* molecular dynamics, a scissor mode of pseudo-water molecules in vibrational spectra was found, which is in well agreement with available experiments.

1. Introduction

Investigation of hydroxylated diamond (0 0 1) surfaces was and remains to be an interesting topic [1–4]. This is because of the excellent chemical, electrical, thermal, mechanical properties, and the good biocompatibility of the diamond. In particular, chemical-vapor deposited (CVD) diamond films have been widely applied for high power electronics, high-temperature semiconductor devices, heat sinks, field effect transistors, optical electronics, Schottky diodes, superhard coatings, as well as biosensing devices [5–9]. In all these applications, surface oxidation is an inevitable issue. The presence of oxygen on the diamond surface can significantly affect the chemical reactivity [10,11], electrical conductivity [12,13], field emission [14,15] and Schottky barrier height [16]. In the early studies, much attention has been given to the oxidation of pristine diamond surfaces [17–21]. However, CVD diamond surfaces are always terminated with hydrogen. Therefore, the investigation of hydrogen and oxygen coexistence on the diamond surfaces could also be important. The presence of the hydroxyl species on diamond surfaces has been demonstrated by organic chemical reactions wetting angle measurements and by XPS [22]. Skokov et al. were the first to systematically study theoretically the oxygenated diamond (0 0 1) surfaces in the presence of hydrogen. They found that the (0 0 1) surfaces containing the hydroxyl groups are energetically more favorable [1]. Using the density-functional theory, Tamura et al. reexamined these surfaces [2]. Their results confirmed that the hydroxylated structures are indeed stable. A parallel arrangement of the OH groups was proposed to be the ground state structure of the OH-network. Later theories, however, questioned this suggestion and suggested instead that the parallel configuration is actually less stable than an anti-parallel (AP) configuration [3,4].

In this paper, we revisit the OH-terminated diamond (0 0 1) surfaces by first-principles calculations. A set of network structures were investigated systemically and two energetically favored structures are found over the reported AP configuration [3]. The transition pathways and barriers between AP and the network structures are also calculated. In addition, using *ab initio* molecular dynamics simulation, a weak scissor mode of water molecule was found in the calculated vibrational spectra. This scissor mode can be understood by the existence of pseudo-water structure.

2. Calculations

We carried out the calculations by using the Vienna *ab initio* simulation package (VASP) [23–25], in which the electron–core interactions were described by the Vanderbilt ultrasoft pseudopotential, [26] and the exchange correlation energy was obtained within the generalized gradient approximation [27]. A plane wave basis set was used to expand the Kohn–Sham orbitals with a 450-eV kinetic energy cutoff. The calculated lattice constant of diamond 3.574 Å is only 0.2% larger than the experimental value of 3.567 Å. To mimic the (0 0 1) surfaces, a supercell approximation was used

* Corresponding author.
E-mail address: hongxin.yang@cea.fr (H.X. Yang).

0039-6028/$ - see front matter © 2009 Elsevier B.V. All rights reserved.
doi:10.1016/j.susc.2009.08.014

in which each slab is separated from the neighboring slabs by about 15 Å of vacuum, and the slab contained 12 layers of carbon atoms. Hydrogen atoms were used to passivate bottom surfaces. The Monkhorst–Pack scheme [28] was used for the Brillouin zone integration, and we used a $2 \times 2 \times 1$ k-point mesh. In the energy minimization, we have allowed for the atoms to fully relax according to the atomic forces, except for those at the bottom two layers, which are fixed at their respective positions of the (2×1) surface. The energy convergence for the structural optimization is better than 0.5 meV/Å. The "climbing image nudged elastic band" method [29] is applied to locate the transition state geometries for calculations of the diffusion barriers. For the vibrational spectra, molecular dynamics (MD) simulations with a time step of 0.5 fs have been run for 2 ps at about 15 K after equilibrating the system for 1 ps.

3. Results and discussions

3.1. Structures and energetics

The OH group terminated diamond (0 0 1) surfaces have been well studied in previous works. The structure with parallel alignment of OH groups, was proposed to be the ground state by Skokov et al. [1] and Tamura et al. [2]. However, the parallel configuration was questioned and found to be less stable than the AP configuration as shown in Fig. 1a. Sque et al. [3] calculated the energy difference between parallel and AP structures of about 85 meV per (2×2) unit cell with LDA calculations, and Yang et al. [4] reported the data is about 250 meV per (2×2) unit cell by using GGA method. They ascribed the energy lowering to the elimination of the polarized electric field energy due to the anti-parallel alignment of the OH groups in the AP structure.

Considering the flexibility of hydrogen bonds, we reexamined these structures, and proposed a set of hydrogen-bonded hydroxyl network structures. Two new structures are found to be much favored over the AP configuration.

3.1.1. Chains with Arm-Chair structure (AC)

The optimized structure of chains with Arm-Chair (AC) is shown in Fig. 1b. In this structure, the OH groups are connected with hydrogen bonds (indicated with red dashed lines), and the hydrogen-bonded chains are along the trench of the (2×1)-reconstructed substrate. The main feature of this topological structure is that it merges the two hydrogen-bonded chains in the AP structure into a single one.

The calculations revealed that, the lengths of hydrogen bonds are 1.52 Å between atoms 2 and 3, and 1.58 Å between atoms 4 and 5, respectively. Both these hydrogen bonds are shorter than the hydrogen bonds in the AP configuration, 1.64 Å. Due to the enhancement of the H-bonds in AC structure the total energy is lower by 104 meV per (2×2) supercell than that of the AP configuration (Fig. 3). This energy difference is a bit smaller than the reported H-bond strength to their corresponding lengths [30]. In the paper of Jones et al., the H-bond strengths (D_E) corresponding to the H-bond lengths (d) follows a power law of the form:

$$D_E = -Ad^{-B} \tag{1}$$

where $A = 18.9$ (13.9) eV and $B = 6.1$ (5.5) from DFT surface (gas-phase) calculations. Using this relationship to estimate the energy difference between AC and AP structures, we get the value of energy difference is 0.78 (0.68) eV/(2×2) supercell, which is larger than our result. This is due to the negligible of effect of the (2×1)-reconstructed diamond substrate, on which there are carbon–carbon π bonds whose strength are comparable with those of H-bonds. The strength of ½ of the carbon–carbon π bond is

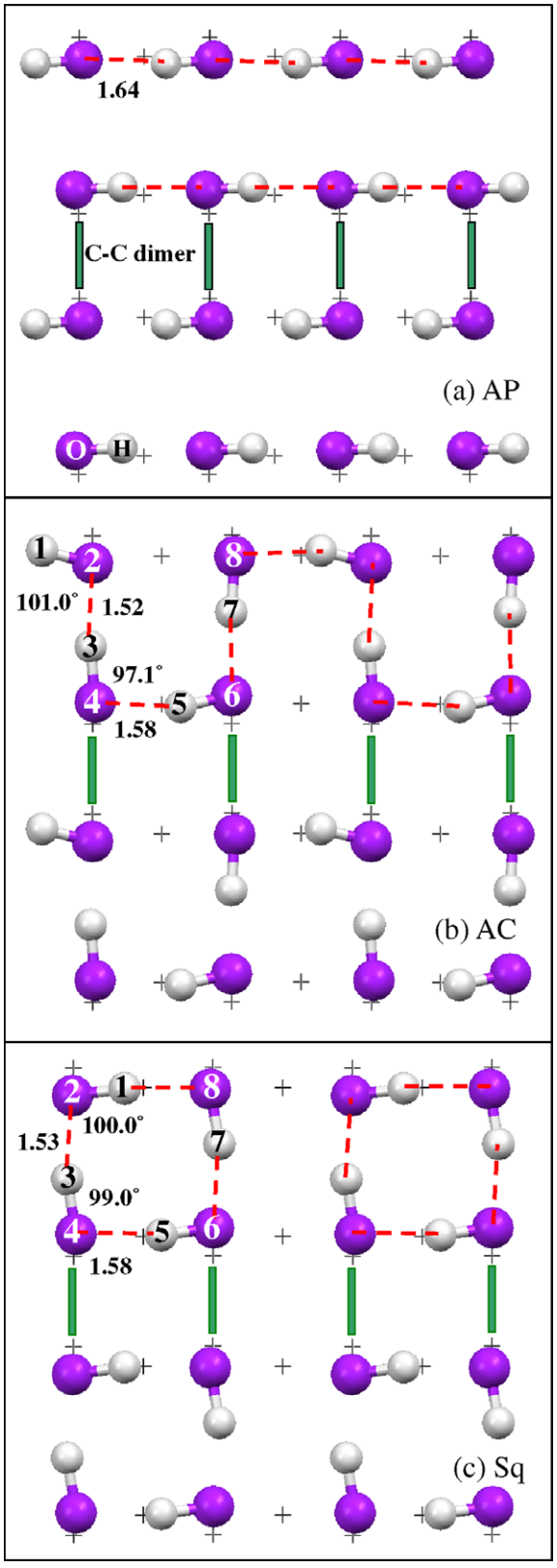

Fig. 1. Top view of the structures for OH-terminated diamond (0 0 1) surfaces: (a) anti-parallel configurations (AP), (b) chains with Arm-Chair (AC), and (c) Square structure (Sq). In this figure and the following figures, the atoms in purple colors are oxygen atoms, and white ones are hydrogen. For clarity, only some of the top two layers of carbon atoms are shown with cross in black. (For interpretation of the references to colour in this figure legend, the reader is referred to the web version of this article.)

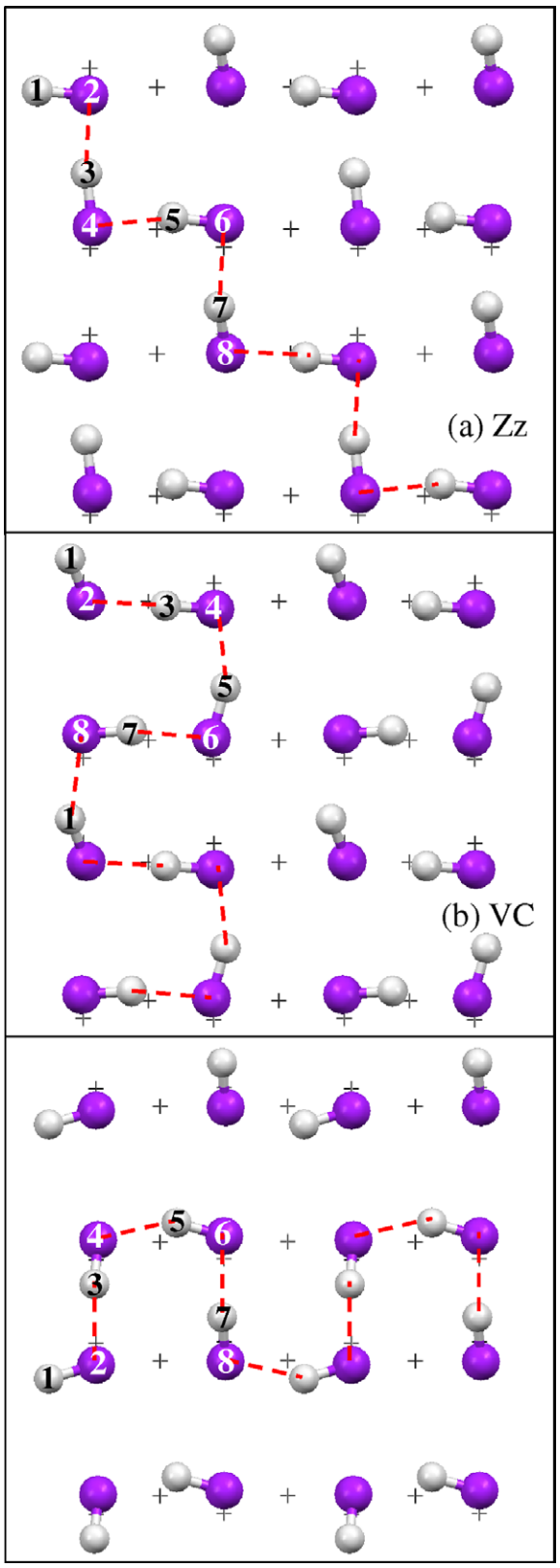

Fig. 2. Top view of the structures for OH-terminated diamond (0 0 1) surfaces: (a) structure with Zigzag chains (Zz), (b) structure with chains Vertical to AC (VC), and (c) structure with chains on Dimer Top (DT).

0.9 eV [31,32]. This value was calculated by using the theoretical cohesive energy of carbon of 10.15 eV [32] and the (1 1 0) surface energy of 3.26 eV [32], assuming that no strained σ bond exists on the (1 1 0) surface.

When the hydrogen bonds formed, the OH groups parallel and vertical to the dimerizations are slightly tilted due to the repulsion between the hydrogens. The angle of H1–O2···H3 is about 101.0°, while the angle of H3–O4···H5 is about 97.1°. Both are larger than 90°, but smaller than the angle of H–O–H in water, 104.5°. [33] Interestingly, due to the strong hydrogen bond between O2 (O4) and H3 (H5), H1–O2···H3 (H3–O4···H5) can be regarded as a water-like structure, named as *pseudo-water*. Their properties will be studied further with vibrational spectra below.

3.1.2. Square configuration (Sq)

Different from the formation of the global network structure of AC, a local network structure named square configuration (Sq) can be formed as shown in Fig. 1c. In one square, four hydrogen bonds are formed such that the opposite hydrogen bond lengths are equal. The lengths of hydrogen bonds are 1.53 Å between atoms 2 and 3, and 1.58 Å between atoms 4 and 5. Both of them are still shorter than the length of hydrogen bonds in the AP configuration. Although the bond lengths remained fairly constant the H1–O2···H3 angle is decreased to about 100.0°, and the H3–O4···H5 angle is increased to about 99.0°. Because of the strengthening of the hydrogen bonds, the total energy of Square structure is lower by about 33 meV per (2×2) supercell than that of the AP configuration. But compared to the AC structure, it is less stable. If considering the relationship between H-bond strengths and their corresponding lengths by using Eq. (1), the energy difference between AC and Sq is 58 meV/(2×2) supercell, which is well consistent to our 71 meV/(2×2) supercell.

3.1.3. Other configurations of network

To investigate more possible lower energy structures that are networked, we also calculated three other possible configurations. First, the structure with Zigzag chains (Zz) is presented in Fig. 2a. The length of hydrogen bond on top of the substrate's trench position between atoms 2 and 3 is strengthened to 1.49 Å, while that between atoms 6 and 7 on top of the C–C dimer is weakened to 1.68 Å. The length of hydrogen bond between atoms 4 and 5 is about 1.54 Å. Here if we taken the Eq. (1) to analysis the H-bond strengths, the energy gain should be 0.71 eV/(2×2) supercell compared to the AP structure. But the total energy of the Zz system is higher for 0.117 eV/(2×2) supercell than that of the AP structure. This is also due to the regardless of the effect of substrate. Then the structure with chains Vertical to AC (VC) is shown in Fig. 2b. The length of hydrogen bond between atoms 4 and 5 on top of the trench is about 1.54 Å, while the length of hydrogen bond between atoms 8 and 1 on top of the dimer is elongated to 1.75 Å. The

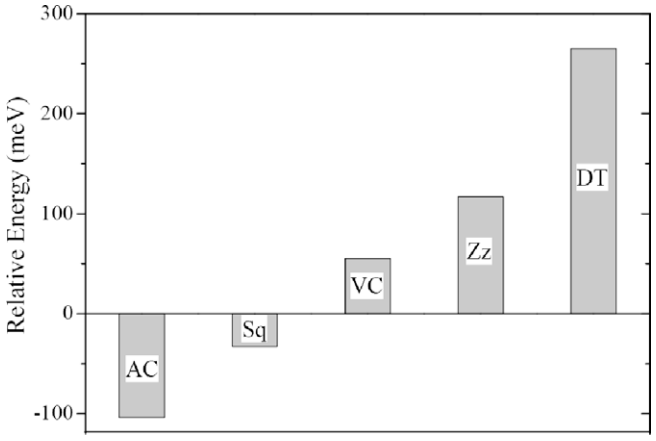

Fig. 3. The relative energies per (2×2) supercell of network structures respect to anti-parallel configuration.

length of hydrogen bond between atoms 2 and 3 is 1.57 Å. For VC structure, the average strength of H-bonds is also enhanced, from the view of Eq. (1), the energy gain should be 0.35 eV/(2 × 2) supercell. While, the total energy calculation revealed that VC is not as stable as AP structure with energy higher for 0.06 eV/(2 × 2) supercell. Finally, we present the structure with chains on the Dimer Top (DT) in Fig. 2c. The length of hydrogen bond between atoms 2 and 3 is about 1.68 Å, and the length of hydrogen bond between atoms 4 and 5 is 1.60 Å. For DT structure, if considering the H-bond strengths corresponding to their lengths, the H-bonds are weakened by 0.024 eV/(2 × 2) supercell, and the total energy calculations show that the energy is higher for 0.265 eV/(2 × 2) supercell than that of AP.

The relative energies of the network structures compared to AP configuration are shown in Fig. 3. The energies of three structures represented in Fig. 2 are all higher than that of the AP structure. This seems not consistent with the relationship between H-bond strengths and their corresponding lengths. While, we think this is due to the negligible of the effect from the flexible π bonds existed on diamond substrate.

3.2. Kinetics

In order to further understand the kinetics characterization of these configurations, we studied systemically the diffusion pathways and barriers from structures with higher energies to the most stable AC structure by using the "climbing image nudged elastic band" method embedded [29] in the VASP code [23–25].

3.2.1. Transitions from Sq to AC and AP to AC

The diffusion pathway from Sq to AC structure is shown in Fig. 4a. The hydrogen atom at position 1 migrates to position 2 by overcoming a barrier of 0.15 eV followed by energy gain of 0.07 eV per (2 × 2) supercell (Fig. 4c).

The transition from AP to AC structure occurs through going the Sq one. First, as shown in Fig. 4b, the hydrogen atom at position 1 (3) migrates to position 2 (4) during the transition from

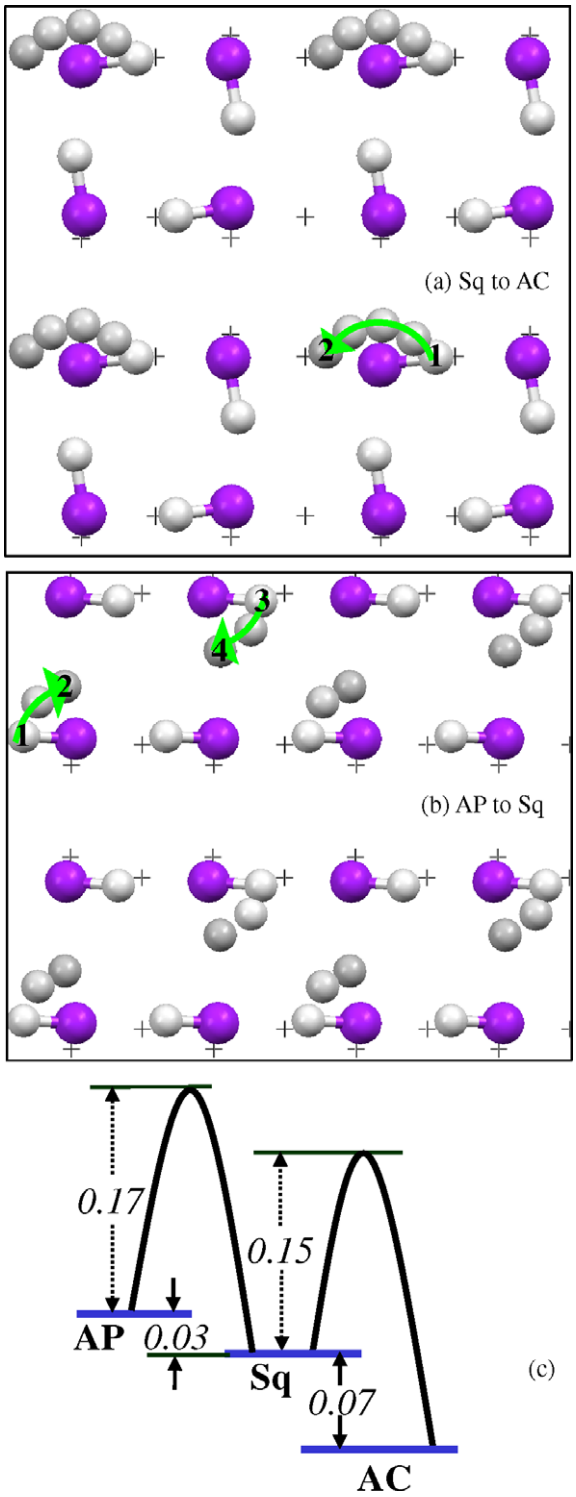

Fig. 4. Top view of pathways for transitions: (a) Sq to AC, and (b) AP to Sq. Their corresponding barriers are shown in panel (c).

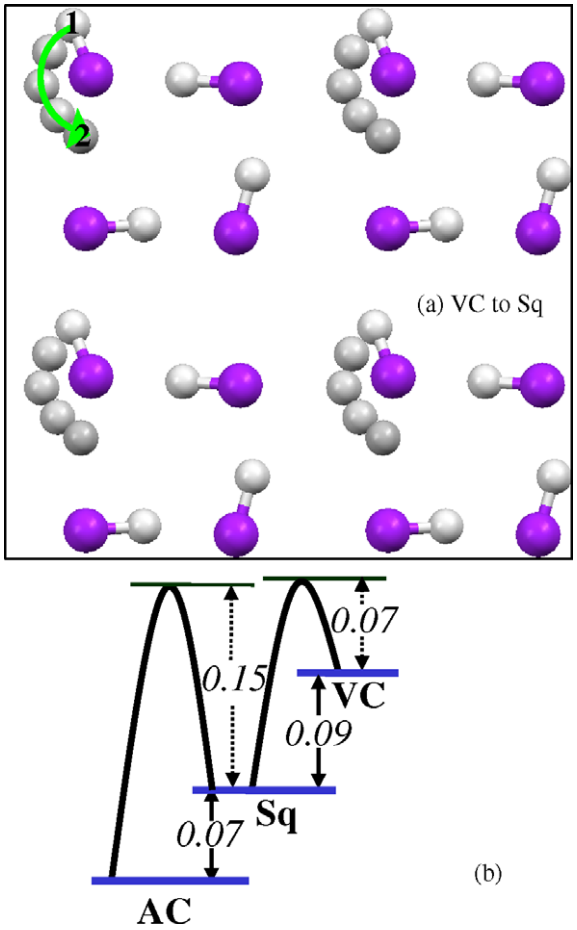

Fig. 5. (a) Top view of the transition pathways of VC to Sq. (b) The transition barriers of VC to Sq and Sq to AC.

AP to Sq. This transition results in energy gain of 0.03 eV per (2×2) supercell after overcoming a barrier of 0.17 eV. Then the transition from Sq to AC occurs the same way described above. One can conclude that the transition from AP to AC is relatively hard due to a high barrier involving complicated migration pathways.

3.2.2. Transition from VC to AC

Similar to the case of AP to AC, the transition from VC to AC occurs through the Sq structure. As shown in Fig. 5, the hydrogen atom at position 1 migrates to position 2 by overcoming a barrier of 0.07 eV followed by energy gain of 0.09 eV. After that, the transition from Sq to AC occurs the way discussed above. Thus, the energy gain for VC to AC transition is found to be 0.16 eV per (2×2) supercell suggesting that the spontaneous transition may be provoked by an initial energy of 0.07 eV.

3.2.3. Transition from Zz to AC

The conversion from Zz to AC structure is the one step process, where the hydrogen atom located at position 1 translates into position 2 (Fig. 6a). The calculated barrier in this case is just 0.06 eV, while energy gain associated with the process is 0.22 eV (Fig. 6b), making this transition highly probable happened.

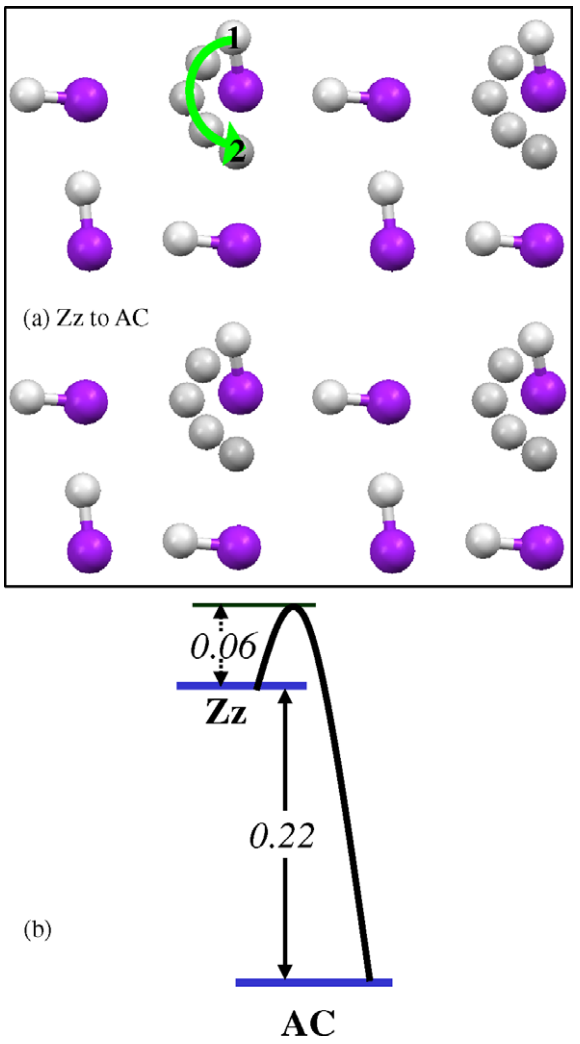

Fig. 6. (a) Top view of the pathway for transition of Zz to AC. (b) The transition barrier of Zz to AC.

3.3. Vibrational spectra

The vibrational spectra for AC structure are represented in Fig. 7b. These spectra were obtained from the velocity autocorrelation function using in the *ab initio* molecular dynamics (MD) simulation data. The trajectories with constant energy have been calculated for 2 ps, with a time step of 0.5 fs, at ~15 K, after equilibrating the system for ~1 ps. The left hand side of the spectra show, two sharp peaks at 36 and 100 meV, as well as three additional modes at 63, 66, and 95 meV. The corresponding vibrational modes in the high resolution electron energy loss spectroscopy (HREELS) spectra (Fig. 7a, Ref. [34]) are in the range of 30–121 meV, and only the peaks at 49, 57, and 108 meV are discernible. On the right hand side of the spectra there are two peaks at 415 meV and 454 meV. Comparing them with the OH stretch frequencies in the gas phase of 454 meV (symmetric) and 466 meV (asymmetric) [35], we note that the OH frequencies are weakened on the diamond (0 0 1) surface and have a red shift due to the formation of H-bond. A broad feature at the center of 433 meV observed in the HREELS spectra experiments [34] may be caused by temperature effects, which makes the two peaks indistinguishable. We believe that this broad feature observed experimentally corresponds to the two modes on the right hand side of Fig. 7b.

More interesting is the peak at 217 meV in the spectra. In this region, the modes of OH vibrational frequencies are OH bending

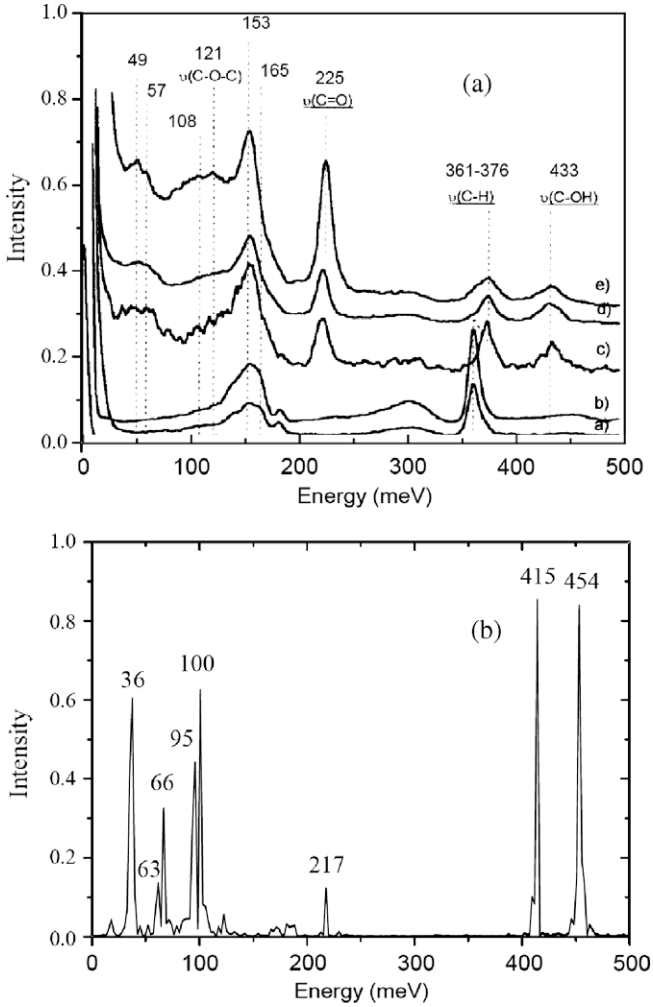

Fig. 7. (a) The spectra taken from Ref. [34] by high resolution electron energy loss spectroscopy for water wetted diamond (0 0 1) surfaces. (b) *Ab initio* MD simulated vibrational spectra for structure of chains with Arm-Chair. A pseudo scissor mode of H–O···H at 217 meV is found.

modes. Similar to the H–O–H scissor modes in the water on a metallic surface (202 meV) [36], the peak at 217 meV in Fig. 7b can be viewed as a pseudo scissor mode of H–O···H. This can be understood from the AC structure shown in Fig. 1b. The hydrogen bond length of O2···H3 is equal to 1.52 Å, making the interaction between the oxygen atom O2 and hydrogen atom H3 very strong. This leads to the formation of pseudo-water structure with the H1–O2···H3 angle of 101.0°, close to that in water, 104.5° [33]. Compared to the H–O–H scissor mode, the pseudo scissor mode of H–O···H has a blueshift in frequency due to faster vibrational motion of H in hydroxyl H–O compared to that in water. However, its intensity is lower because H bond in pseudo-water is weaker than the OH bond in water. We thought the experimental mode at 225 meV in Fig. 7a which is assigned to the C=O vibration should be the pseudo scissor one.

4. Conclusions

A set of network structures for hydroxyl on diamond (0 0 1) surfaces are investigated via *ab initio* calculations. Arm-Chair and Square structures are found to be more stable than the recent reported anti-parallel configuration. The transition pathways and barrier values between these structures are also studied. Furthermore, the vibrational spectra of the stable structures were studied by *ab initio* MD simulations. A scissor mode at 217 meV was found, which can be used to identify the network type structures. The value of the mode agrees with the one observed at in experiments.

Acknowledgements

This work was supported by the National Natural Science Foundation of China (10634070, 10774177, 50672121 and 50825206), and the Chair d'Excellence Program of Nanosciences Foundation of Grenoble, France.

References

[1] S. Skokov, B. Weiner, M. Frenklach, Phys. Rev. B 55 (1997) 1895.
[2] H. Tamura, H. Zhou, K. Sugisako, Y. Yokoi, S. Takami, M. Kubo, K. Tersishi, A. Miyamoto, A. Imamura, M.N. Gamo, T. Ando, Phys. Rev. B 61 (2000) 11025.
[3] S.J. Sque, R. Jones, P.B. Briddon, Phys. Rev. B 73 (2006) 085313.
[4] H.X. Yang, L.F. Xu, C.Z. Gu, S.B. Zhang, Appl. Surf. Sci. 253 (2007) 4260.
[5] J. Isberg, J. Hammersberg, E. Johansson, T. Wikström, D.J. Twitchenm, A.J. Whitehead, S.E. Coe, G.A. Scarsbrook, Science 297 (2002) 1670.
[6] D.M. Gruen, MRS Bull. 26 (2001) 771.
[7] S. Koizumi, K. Watanabe, M. Hasegawa, H. Kanda, Science 292 (2001) 1899.
[8] A. Aleksov, A. Denisenko, M. Kunze, A. Vescan, A. Bergmaier, G. Dollinger, W. Ebert, E. Kohn, Semicond. Sci. Technol. 18 (2003) S59.
[9] H. Kawarada, Y. Araki, T. Sakai, T. Ogawa, H. Umezawa, Phys. Status Solidi A 185 (2001) 79.
[10] J.S. Foord, L.C. Hian, R.B. Jackman, Diam. Relat. Mater. 10 (1996) 710.
[11] H. Notsu, I. Yagi, T. Tatsuma, D.A. Tryk, A. Fujishima, J. Electroanal. Chem. 492 (2000) 31.
[12] J. Shirafuji, T. Sugino, Diam. Relat. Mater. 5 (1996) 706.
[13] J.S. Foord, C.H. Lau, M. Hiramatsu, R.B. Jackman, C.E. Nebel, P. Bergonzo, Diam. Relat. Mater. 11 (2002) 856.
[14] T. Yamada, T. Yokoyama, A. Sawabe, Diam. Relat. Mater. 11 (2002) 780.
[15] J.I.B. Wilson, J.S. Walton, G. Beamson, J. Electron, Spectrosc. Relat. Phenom. 121 (2001) 183.
[16] C. Saby, P. Muret, Diam. Relat. Mater. 11 (1996) 851.
[17] P. Bdazing, W.S. Verwoerd, Surf. Sci. 183 (1987) 469.
[18] N. Russo, in: C. Morterra, A. Zecchina, G. Costa (Eds.), Structure and Reactivity of Surfaces, Elsevier, Amsterdam, 1989, p. 809.
[19] X.M. Zheng, P.W. Smith, Surf. Sci. 262 (1992) 219.
[20] S. Skokov, B. Weiner, M. Frenklach, Phys. Rev. B 49 (1994) 11374.
[21] J.L. Whitten, P. Cremashi, R.E. Thomas, R.A. Rudder, R.J. Markunas, Appl. Surf. Sci. 75 (1994) 45.
[22] R. Boukherroub, X. Wallart, S. Szunerits, B. Marcus, P. Bouvier, M. Mermoux, Electrochem. Commun. 7 (2005) 937.
[23] G. Kresse, J. Hafner, Phys. Rev. B 47 (1993) 558.
[24] G. Kresse, J. Furthmüller, Phys. Rev. B 54 (1996) 11169.
[25] G. Kresse, J. Furthmüller, Comput. Mater. Sci. 6 (1996) 15.
[26] D. Vanderbilt, Phys. Rev. B 41 (1990) 7892.
[27] Y. Wang, J.P. Perdew, Phys. Rev. B 44 (1991) 13298.
[28] H.J. Monkhorst, J.D. Pack, Phys. Rev. B 13 (1976) 5188.
[29] H. Jónsson, G. Mills, K.W. Jacobsen, in: B.J. Berne et al. (Eds.), Classical and Quantum Dynamics in Condensed Phase Simulations, World Scientific, Singapore, 1998;
G. Henkelman, B.P. Uberuaga, H. Jónsson, J. Chem. Phys. 113 (2000) 9901.
[30] G. Jones, S.J. Jenkins, D.A. King, Surf. Sci. 600 (2006) L224.
[31] H.X. Yang, L.F. Xu, Z. Fang, C.Z. Gu, S.B. Zhang, Phys. Rev. Lett. 100 (2008) 026101.
[32] A.A. Stekolnikov, J. Furthmüller, F. Bechstedt, Phys. Rev. B 65 (2002) 115318.
[33] W.S. Benedict, N. Gailer, E.K. Plyler, J. Chem. Phys. 59 (1973) 2254.
[34] P.E. Pehrsson, T.W. Mercer, Surf. Sci. 460 (2000) 74.
[35] F. Sim, St-Amant Alain, I. Papai, D.R. Salahub, J. Am. Chem. Soc. 114 (1992) 4391.
[36] S. Meng, L.F. Xu, E.G. Wang, S. Gao, Phys. Rev. Lett. 89 (2002) 176104.